Inorg. Chem. **2007**, *46*, 11243–11253

Self-Assembled Metallacycles with Pyrazine Edges: A New Example in Which the *Unexpected* Molecular Triangle Prevails over the *Expected* Molecular Square

Sofia Derossi,[†,‡] Massimo Casanova,[†] Elisabetta Iengo,[†,§] Ennio Zangrando,*[,†] Mauro Stener,[†] and Enzo Alessio*[,†]

Dipartimento di Scienze Chimiche, Università di Trieste, Via L. Giorgieri 1, 34127 Trieste, Italy

Received October 2, 2007

The combination of cis-protected metal fragments with linear linkers is expected to yield molecular squares. We found instead that treatment of the 90° angular precursor *trans*-[$RuCl_2$(dmso–S)$_4$] (**1**) with an equivalent amount of the linear and rigid pyrazine (pyz) linker unexpectedly yields, in a number of different experimental conditions, the molecular triangle [{*trans,cis*-$RuCl_2$(dmso–S)$_2$(μ-pyz)}$_3$] (**3**), together with polymeric material. Very similar results were also obtained from the reaction between **1** and the preformed corner fragment *trans,cis,cis*-[$RuCl_2$(dmso–S)$_2$(pyz)$_2$] (**6**). In both cases, the expected molecular square [{*trans,cis*-$RuCl_2$(dmso–S)$_2$(μ-pyz)}$_4$] (**4**) was observed only as a transient species. These results suggest that **3**, which is the first example of a *neutral* molecular triangle with octahedral metal corners and pyrazine edges, is both the thermodynamic and the kinetic product of the reactions described above. The X-ray structure of **3** shows that the main distortions from ideal coordination geometry concern the N–Ru–N angles, which are narrower than 90°, and the coordination bonds of pyz. The pyrazine molecules, which are basically planar, are significantly tilted from linearity. Calculations performed on **6** indicated that the N–Ru–N angle is ca. six times more rigid than the tilt angle of pyrazine. The structural and theoretical findings on **3** and **6**, together with the previous examples of molecular triangles and squares with cis-protected metal corners and linear pyz edges, suggest that the entropically favored molecular triangles might be preferred over the expected molecular squares with metal corner fragments that spontaneously favor N_{pyz}–M–N_{pyz} angles narrower than 90° because of the presence of ancillary ligands with significant steric demand on the coordination plane. The rather-flexible coordination geometry of pyrazine can accommodate the moderate distortions from linearity required to close the small metallacycle with modest additional strain.

Introduction

The metal-mediated rational construction of discrete molecular assemblies is one of the thriving areas of supramolecular chemistry.[1] Many examples of structurally fascinating compounds have been designed and prepared according to this synthetic paradigm, and some of them are finding applications as receptors and molecular vessels for trapping reactive intermediates[2] and for stoichiometric[3] and catalytic reactions.[4]

Perhaps the most simple among all of the metal-directed self-assembly processes is the combination of a 90° angular cis bis-acceptor metal fragment with an equimolar amount of a linear linker. According to the *directional bonding*

* To whom correspondence should be addressed. E-mail: alessi@units.it.
† Università di Trieste.
‡ Current address: Department of Chemistry, University of Sheffield, Sheffield, UK S3 7HF.
§ Current address: University of Cambridge, Chemical Laboratories, Lensfield Road, Cambridge CB2 1EW, UK.

(1) Fujita, M. *Chem. Soc. Rev.* **1998**, *27*, 417−425. (b) Olenyuk, B.; Fechtenkötter, A.; Stang, P. J. *J. Chem. Soc., Dalton Trans.* **1998**, 1707−1728. (c) Caudler, D. L.; Raymond, K. N. *J. Chem. Soc., Dalton Trans.* **1999**, 1185−1200. (d) Navarro, J. A. R.; Lippert, B. *Coord. Chem. Rev.* **2001**, *222*, 219−250. (e) Paul, R. L.; Bell, Z. R.; Jeffrey, J. C.; McCleverty, J. A.; Ward, M. D. *Proc. Natl. Acad. Sci. U.S.A.* **2002**, *99*, 4883−4888.

(2) Yoshizawa, M.; Kusukawa, T.; Fujita, M.; Yamaguchi, K. *J. Am. Chem. Soc.* **2000**, *122*, 6311−6312. (b) Yoshizawa, M.; Kusukawa, T.; Fujita, M.; Sakamoto, S.; Yamagichi, K. *J. Am. Chem. Soc.* **2001**, *123*, 10454−10459.

(3) Yoshizawa, M.; Takeyama, Y.; Kusukawa, T.; Fujita, M. *Angew. Chem., Int. Ed.* **2002**, *41*, 1347−1349.

(4) Fiedler, D.; van Halbeek, H.; Bergman, R. G.; Raymond, K. N. *J. Am. Chem. Soc.* **2006**, *128*, 10240−10252. (b) Yoshizawa, M.; Tamura, M.; Fujita, M. *Science* **2006**, *312*, 251−254. (c) Pluth, M. D.; Bergman, R. G.; Raymond, K. N. *Science* **2007**, *316*, 85−88.

10.1021/ic7019507 CCC: $37.00
Published on Web 11/10/2007

Scheme 1. Self-Assembly of a 90° Angular Metal Fragment with a Linear Linker to Yield a Molecular Square

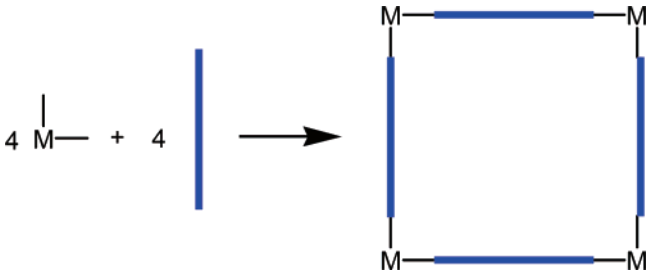

approach by Holliday and Mirkin[5] (previously defined as the *molecular library model* by Stang and co-workers[6]) this combination should, *in principle*, lead selectively to the corresponding 4 + 4 molecular square (Scheme 1).

This was actually found by Fujita and co-workers in 1990 when they described the selective preparation of the molecular square $[\{Pd(en)(\mu\text{-}4,4'\text{-bipy})\}_4](NO_3)_8$ by the self-assembly of $Pd(en)(NO_3)_2$ (en = ethylenediammine) and 4,4′-bipy (4,4′-bipy = 4,4′-bipyridine), in what is universally recognized as the first example of a rationally designed metallacycle.[7] However, the outcome of this apparently straightforward self-assembly reaction is indeed scarcely predictable, also with simple linkers such as 4,4′-bipy.[8,9] There are indeed several examples in which the directional preference of the components is not fulfilled and the combination of predetermined linear linkers and 90° angular metal fragments leads to mixtures of molecular squares and molecular triangles, which may,[8−15] or may not,[16,17] be in equilibrium (Scheme 2).

In some cases, the formation of triangles occurs exclusively.[18−26] In others, molecular triangles are found in the solid state, and it is unclear what species occur in solution.[27,28]

It is recognized that several factors play a role in affecting the square/triangle preference: solvent, temperature, reagents

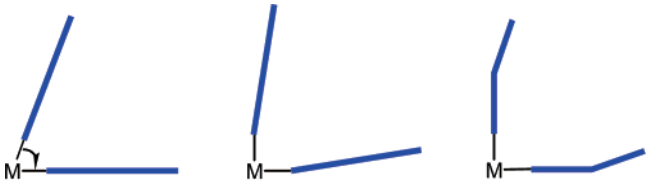

Figure 1. Schematic representation of the main distortions that may occur in the formation of a molecular triangle from a 90° angular metal fragment and a linear linker; coordination angle (left), coordination geometry (center), bending of the linker (right).

ratio, nature of the metal center, nature of the ancillary ligands on the metal fragments, and nature of the linkers (even small variations within the same class of ligand can lead to different products),[8−15,29−32] but the role of each factor is far from being well understood. On the other hand, it is normally accepted that the formation of a triangle is favored for entropic reasons (assembly of six rather than eight fragments), whereas it is disfavored by enthalpic considerations because some distortions *must* obviously occur upon closure of the small metallacycle, leading to strain. In particular, one or more of the following distortions are expected: (*i*) coordination angles smaller than 90°, (*ii*) nonlinear coordination geometries, and (*iii*) connectors being distorted from linearity to some extent (Figure 1).

For this last reason, molecular triangles are expected to be favored over the corresponding squares when extended and constitutionally flexible linkers are employed:[8] small distortions of bond angles that lead to deviations from linearity will be easily distributed along the frame of the ligand without much enthalpic loss.

As a consequence, pyrazine (pyz), which is the shortest and stiffest linear aromatic nitrogen linker, would be expected to give molecular squares exclusively, when combined with 90° cis bis-acceptor metal fragments. Indeed there are in the literature several examples of structurally characterized molecular squares, both cationic and neutral, having pyz molecules as edges and a variety of metal ions as corners: Pt(II),[33,34] Re(I),[35,36] Ru(II/III),[37] and Ti(II).[38] Surprisingly,

(5) Holliday, B. J.; Mirkin, C. A. *Angew. Chem., Int. Ed.* **2001**, *40*, 2022−2043.
(6) Leininger, S.; Olenyuk, B.; Stang, P. *J. Chem. Rev.* **2000**, *100*, 853−908.
(7) Fujita, M.; Yazaki, J.; Ogura, K. *J. Am. Chem. Soc.* **1990**, *112*, 5645−47.
(8) Fujita, M.; Sasaki, O.; Mitsuhashi, T.; Fujita, T.; Yazaki, J.; Yamaguchi, K. *Chem. Commun.* **1996**, 1535−1536.
(9) Uehara, K.; Kasai, K.; Mizuno, N. *Inorg. Chem.* **2007**, *46*, 2563−2570.
(10) Lee, S. B.; Hwang, S.; Chung, D. S.; Yun, H.; Hong, J.-I. *Tetrahedron Lett.* **1998**, *39*, 873−876.
(11) Sautter, A.; Schmid, D. G.; Jung, G.; Würthner, F. *J. Am. Chem. Soc.* **2001**, *123*, 5424−30.
(12) Schweiger, M.; Russell Seidel, S.; Arif, A. M.; Stang, P. J. *Inorg. Chem.* **2002**, *41*, 2556−2559.
(13) Ferrer, M.; Mounir, M.; Rossell, O.; Ruiz, E.; Maestro, M. A. *Inorg. Chem.* **2003**, *42*, 5890−5899. b) Ferrer, M.; Rodriguez, L.; Rossell, O. *J. Organomet. Chem.* **2003**, *681*, 158−166.
(14) Cotton, F. A.; Murillo, C. A.; Yu, R. *Dalton Trans.* **2006**, 3900−3905.
(15) Ferrer, M.; Gutiérrez, A.; Mounir, M.; Rossell, O.; Ruiz, E.; Rang, A.; Engeser, M. *Inorg. Chem.* **2007**, *46*, 3395−3406.
(16) McQuillan, F. S.; Berridge, T. E.; Chen, H.; Hamor, T. A.; Jones, C. J. *Inorg. Chem.* **1998**, *37*, 4959−4970.
(17) Yu, S.-Y.; Huang, H.-P.; Li, S.-H.; Jiao, Q.; Li, Y.-Z.; Wu, B.; Sei, Y.; Yamaguchi, K.; Pan, Y.-J.; Ma, H.-W. *Inorg. Chem.* **2005**, *41*, 9471−9488.
(18) Schnebeck, R.-D.; Randaccio, L.; Zangrando, E.; Lippert, B. *Angew. Chem., Int. Ed.* **1998**, *37*, 119−121.
(19) Neels, A.; Stoeckli-Evans, H. *Inorg. Chem.* **1999**, *38*, 6164−6170.
(20) Yu, X.-Y.; Maekawa, M.; Kondo, M.; Kitagawa, S.; Jin, G.-X. *Chem. Lett.* **2001**, 168−169.
(21) Schweiger, M.; Russell Seidel, S.; Arif, A. M.; Stang, P. J. *Angew. Chem., Int. Ed.* **2001**, *40*, 3467−3469.
(22) Cotton, F. A.; Lin, C.; Murillo, C. A. *Inorg. Chem.* **2001**, *40*, 575−577.
(23) Cotton, F. A.; Daniels, L. M.; Lin, C.; Murillo, C. A. *J. Am. Chem. Soc.* **1999**, *121*, 4538−4539.
(24) Bera, J. K.; Angaridis, P.; Cotton, F. A.; Petrukhina, M. A.; Fanwick, P. E.; Walton, R. A. *J. Am. Chem. Soc.* **2001**, *123*, 1515−1516.
(25) Cotton, F. A.; Murillo, C. A.; Wang, X.; Yu, R. *Inorg. Chem.* **2004**, *43*, 8394−8403.
(26) Cotton, F. A.; Murillo, C. A.; Stiriba, S.-E.; Wang, X.; Yu, R. *Inorg. Chem.* **2005**, *44*, 8223−8233.
(27) Qin, Z.; Jennings, M. C.; Puddephatt, R. J. *Chem. Commun.* **2001**, 2676−2677.
(28) Qin, Z.; Jennings, M. C.; Puddephatt, R. J. *Inorg. Chem.* **2003**, *42*, 1956−1965.
(29) Cotton, F. A.; Daniels, L. M.; Lin, C.; Murillo, C. A. *J. Am. Chem. Soc.* **1999**, *121*, 4538−4539.
(30) Sun, S.-S.; Lees, A. J. *Inorg. Chem.* **1999**, *38*, 4181−4182. (b) Sun, S.-S.; Lees, A. J. *J. Am. Chem. Soc.* **2000**, *122*, 8956−8967.
(31) Berben, L. A.; Faia, M. C.; Crawford, N. R. M.; Long, J. R. *Inorg. Chem.* **2006**, *45*, 6378−6386.
(32) Cotton, F. A.; Liu, C. Y.; Murillo, C. A.; Wang, X. *Inorg. Chem.* **2006**, *45*, 2619−2626.

Scheme 2. Self-Assembly of a 90° Angular Metal Fragment with a Linear Linker to Yield a Mixture of Molecular Squares *and* Molecular Triangles

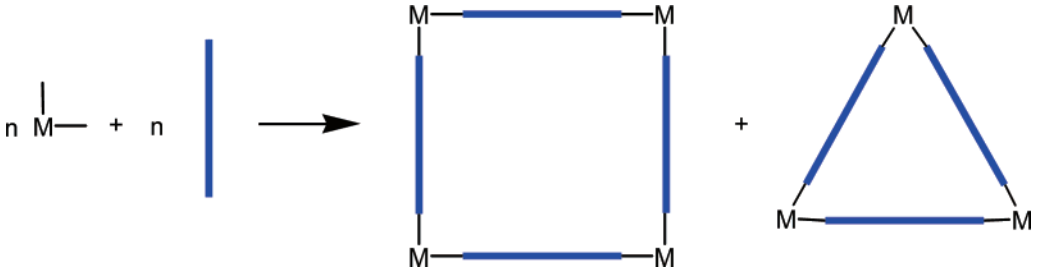

Scheme 3. Reaction of *trans*-[$RuCl_2$(dmso−S)$_4$] (**1**) with an Equimolar Amount of Pyrazine (pyz) Yielding the Neutral Molecular Triangle [{*trans*,*cis*-$RuCl_2$(dmso−S)$_2$(μ-pyz)}$_3$] (**3**)

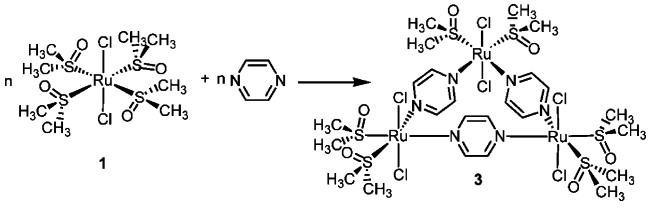

however, there are also two examples in which the combination of pyrazine with cis-protected square-planar metal fragments yields the corresponding molecular triangles *exclusively*: [{$Rh(PPh_3)_2$(μ-pyz)}$_3$](ClO_4)$_3$[20] and [{$Pt(PEt_3)_2$-(μ-pyz)}$_3$](CF_3SO_3)$_6$.[21]

Intrigued by these results, we decided to investigate the reactivity of the Ru(II)−dmso compounds *trans*-[$RuCl_2$-(dmso−S)$_4$] (**1**) and *trans*,*cis*,*cis*-[$RuCl_2(CO)_2$(dmso-O)$_2$] (**2**) toward pyrazine. We have shown that these complexes, after the dissociation of two cis-coordinated sulfoxides, lead selectively and under mild conditions to the highly symmetrical 90° cis bis-acceptor neutral fragments *trans*,*cis*-[$RuCl_2$(dmso−S)$_2$] and *trans*,*cis*-[$RuCl_2(CO)_2$], respectively.[39] By exploiting the binding properties of **1** and **2**, we prepared a series of new ruthenium-mediated assemblies of pyridylporphyrins. The X-ray structures of many of these supramolecular assemblies, including metallacycles and molecular sandwiches of porphyrins, were determined.[40]

Here, we report that combination of *trans*-[$RuCl_2$(dmso−S)$_4$] and pyz leads to the selective formation of the neutral molecular triangle [{*trans*,*cis*-$RuCl_2$(dmso−S)$_2$(μ-pyz)}$_3$] (**3**), rather than the anticipated molecular square (Scheme 3). We also report a detailed discussion, supported by the X-ray structures of **3** and of the corner complex *trans*,*cis*-[$RuCl_2$-(dmso−S)$_2$(pyz)$_2$] (**6**), and by theoretical calculations, on the reasons for this preference.

Experimental Section

Materials. All of the reagents and solvents were used without further purification. The precursors *trans*-[$RuCl_2$(dmso−S)$_4$] (**1**) and *trans*,*cis*,*cis*-[$RuCl_2$(dmso-O)$_2(CO)_2$] (**2**) were prepared following published procedures.[41,42]

Instrumental Methods. ^{1}H NMR spectra were recorded at 400 MHz on a JEOL Eclipse 400FT spectrometer. All of the spectra were run at room temperature, unless stated otherwise. ^{1}H chemical shifts in $CDCl_3$ were referenced to the peak of a residual non-deuterated solvent (δ = 7.26). Infrared spectra were recorded on a PerkinElmer 983G spectrometer. UV−vis spectra were obtained on a Jasco V-500 UV−vis spectrophotometer. Elemental analysis was performed at the Dipartimento di Scienze Chimiche, University of Trieste. The reactions between **1** and pyrazine were monitored over time by ^{1}H NMR spectroscopy with the following procedure: 1 mL samples were periodically withdrawn from the solution, immediately rotary-evaporated to an oil, redissolved in $CDCl_3$, and the NMR spectrum was immediately registered.

Synthesis of the Complexes. [{*trans*,*cis*-$RuCl_2$(dmso−S)$_2$(μ-pyz)}$_3$] (3). To a yellow-orange solution of *trans*-[$RuCl_2$(dmso−S)$_4$] (**1**) (203.0 mg, 0.41 mmol) in chloroform (5 mL), an equimolar amount of pyrazine (33.4 mg, 0.41 mmol) was added. Within a few minutes, the solution turned deep red. A ruby-red precipitate formed overnight at room temperature and was removed by filtration. Addition of methanol to the mother liquor induced the precipitation of an orange-red solid, which was filtered off and thoroughly washed with methanol. For further purification, the solid was redissolved in a minimum amount of chloroform, rapidly filtered over celite to remove small amounts of residual solid, and finally rotary-evaporated to dryness. The dry solid was pure **3** according to ^{1}H NMR analysis. Yield: 75 mg (45%). Anal. Calcd for $C_{24}H_{48}N_6Cl_6O_6Ru_3S_6$ (M_r 1224.95): C, 23.5; H, 3.95; N, 6.86. Found: C, 23.9; H, 4.02; N, 6.93. ^{1}H NMR ($CDCl_3$, δ ppm): 9.37 (s, 12H, pyz), 3.31 (s, 36H, dmso−S). UV−vis spectrum in $CHCl_3$ (λ_{max}, nm): 375, 450 (sh). Crystals of **3** suitable for X-ray investigation were obtained from a chloroform solution by slow diffusion of *n*-hexane.

***trans*,*cis*,*cis*-[$RuCl_2$(dmso−S)$_2$(pyz)$_2$] (6).** To a yellow-orange solution of *trans*-[$RuCl_2$(dmso−S)$_4$] (**1**) (203.0 mg, 0.41 mmol) in chloroform (10 mL), a 20-fold molar excess of pyrazine (652.4 mg, 8.2 mmol) was added. After standing overnight at room

(33) Kumazawa, K.; Biradha, K.; Kusukawa, T.; Okano, T.; Fujita, M. *Angew. Chem., Int. Ed.* **2003**, *42*, 3909−3913.
(34) Willermann, M.; Mulcahy, C.; Sigel, R. K. O.; Cerdà, M. M.; Freisinger, E.; Miguel, P. J. S.; Roitzsch, M.; Lippert, B. *Inorg. Chem.* **2006**, *45*, 2093−2099.
(35) Slone, R. V.; Hupp, J. T.; Stern, C. L.; Albrecht-Schmitt, T. E. *Inorg. Chem.* **1996**, *35*, 4096−4097.
(36) Rajendran, T.; Manimaran, B.; Lee, F.-Y.; Chen, P.-J.; Lin, S.-C.; Lee, G.-H.; Peng, S.-M.; Chen, Y.-J.; Lu, K.-L. *J. Chem. Soc., Dalton Trans.* **2001**, 3346−3351.
(37) Lau, V. C.; Berben, L. A.; Long, J. R. *J. Am. Chem. Soc.* **2002**, *124*, 9042−9043.
(38) Kraft, S.; Beckhaus, R.; Haase, D.; Saak, W. *Angew. Chem., Int. Ed.* **2004**, *43*,1583−1587. (b) Kraft, S.; Hanuschek, E.; Beckhaus, R.; Haase, D.; Saak, W.−*Chem. Eur. J.* **2005**, *11*, 969−978.
(39) Alessio, E. *Chem. Rev.* **2004**, *104*, 4203−4242.
(40) Iengo, E.; Milani, B.; Zangrando, E.; Geremia, S.; Alessio, E. *Angew. Chem., Int. Ed.* **2000**, *39*, 1096−1099. (b) Iengo, E.; Zangrando, E.; Minatel, R.; Alessio, E. *J. Am. Chem. Soc.* **2002**, *124*, 1003−1013. (c) Scandola, F.; Chiorboli, C.; Prodi, A.; Iengo, E.; Alessio, E. *Coord. Chem. Rev.* **2006**, *250*, 1471−1496. (c) Iengo, E.; Scandola, F.; Alessio, E. *Struct. Bonding* **2006**, *121*, 105−144. (d) Iengo, E.; Zangrando, E.; Alessio, E. *Acc. Chem. Res.* **2006**, *39*, 841−851.
(41) Alessio, E.; Mestroni, G.; Nardin, G.; Attia, W. M.; Calligaris, M.; Sava, G.; Zorzet, S. *Inorg. Chem.* **1988**, *27*, 4099−4106.
(42) Alessio, E.; Milani, B.; Bolle, M.; Mestroni, G.; Faleschini, P.; Todone, F.; Geremia, S.; Calligaris, M. *Inorg. Chem.* **1995**, *34*, 4722−4734.

Table 1. Crystallographic Data and Details of Refinements for **3**, **6**, and **7**

compound	**3**.3.5($CHCl_3$)	**6**	**7**
empirical formula	$C_{27.5}H_{51.5}Cl_{16.5}N_6O_6Ru_3S_6$	$C_{12}H_{20}Cl_2N_4O_2RuS_2$	$C_{10}H_8Cl_2N_4O_2Ru$
fw, g mol^{-1}	1642.74	488.41	388.17
T, K	100(2)	293(2)	293(2)
wavelength, Å	1.00000	0.71073	1.54178
cryst syst	monoclinic	monoclinic	orthorhombic
space group	$P2_1/n$	$P2_1/c$	*Pbca*
a, Å	14.222(2)	8.996(3)	9.635(2)
b, Å	21.631(4)	11.221(3)	16.181(3)
c, Å	24.221(4)	19.466(4)	18.170(4)
β, deg	105.53(9)	96.32(2)	
V, $Å^3$	7179(2)	1953.0(9)	2832.8(10)
Z	4	4	8
D_{calcd}, g cm^{-3}	1.520	1.661	1.820
μ (Mo−Kα), mm^{-1}	4.021	1.301	12.478
F(000)	3260	984	1520
θ range, deg	2.48−30.18	2.91−27.48	5.87−64.64
no. collected data	39 719	22 307	21 531
unique data	7255	4058	2307
R_{int}	0.0215	0.0631	0.0470
data, $I > 2\sigma(I)$	6341	2389	1931
refined params	599	212	173
R1[a] [$I > 2\sigma(I)$]	0.0613	0.0348	0.0608
wR2[a] [$I > 2\sigma(I)$]	0.1784	0.0693	0.1538
GOF[b]	1.163	0.824	1.092
residuals, e $Å^{-3}$	1.922, −1.023	0.444, −0.363	1.110, −1.160

[a] $R1 = \sum||F_o| - |F_c||/\sum|F_o|$, $wR2 = [\sum w(F_o^2 - F_c^2)^2/\sum w(F_o^2)^2]^{1/2}$. [b] $GOF = \{\sum[w(F_o^2 - F^{c2})^2]/(n - p)\}^{1/2}$.

temperature, during which time the solution turned deep red, the solvent was rotary-evaporated. Addition of 1 mL of acetone to the remaining oil induced the rapid formation of deep-red crystals (suitable for X-ray investigation) that were removed by filtration, rapidly washed with cold acetone and diethyl-ether, and vacuum-dried at room temperature. Yield 140.2 mg (70%). Anal. Calcd for $C_{12}H_{20}N_4Cl_2O_2RuS_2$ (M_r 488.40): C, 29.5; H, 4.13; N, 11.5. Found: C, 29.4; H, 4.05; N, 11.4. ^{1}H NMR ($CDCl_3$, δ ppm): 9.29 (d, 4H, H2,6), 8.57 (d, 4H, H3,5), 3.28 (s, 12H, dmso−S). Selected IR (KBr, cm^{-1}): $\nu_{S=O}$ 1097 (vs); ν_{Ru-S} 425 (m); ν_{Ru-Cl} 341 (m). UV−vis spectrum in $CHCl_3$ (λ_{max}, nm): 320 (with very broad tail that covers all of the visible range).

***trans,cis,cis*-[$RuCl_2(CO)_2(pyz)_2$] (7).** To a yellow solution of *trans,cis,cis*-[$RuCl_2$(dmso-O)$_2(CO)_2$] (**2**) (103.0 mg, 0.27 mmol) in chloroform (2 mL), a 20-fold molar excess of pyrazine (430.0 mg, 5.4 mmol) was added. Small crystals of the product precipitated spontaneously from the solution after a few days at ambient temperature; the amount of precipitate was increased by the gradual addition of ca. 2 mL of diethyl ether (over 3 days). The yellow crystals were collected by filtration, washed with cold methanol and diethyl ether, and vacuum-dried at room temperature. Yield 70 mg (67%). Anal. Calcd for $C_{10}H_8N_4Cl_2O_2Ru$ (M_r 388.17): C, 30.9; H, 2.07; N, 14.4. Found: C, 31.1; H, 2.04; N, 14.3. ^{1}H NMR ($CDCl_3$, δ ppm): 9.00 (d, 4H, H2,6), 8.80 (d, 4H, H3,5). Selected IR (KBr, cm^{-1}): $\nu_{C=O}$ 2071 (s), 2003 (vs); ν_{Ru-Cl} 339 (m).

Crystallographic Measurements. Crystal data and details of data collections and refinements for the structures reported are summarized in Table 1. Diffraction data for the structure of **3** were collected at the X-ray diffraction beamline of the Elettra Synchrotron, Trieste (Italy), using the rotating crystal method with a monochromatic wavelength of 1.0 Å. Data were collected on a CCD MAR detector. Measurements were performed at 100 K using a nitrogen stream cryo-cooler. Data collection of **6** and of **7** were carried out on a Nonius DIP-1030H system (Mo Kα radiation, $\lambda = 0.71073$ Å) and on a Bruker Kappa CCD imaging plate mounted on a Nonius FR591 rotating anode ($\lambda = 1.54178$ Å), respectively. Cell refinement, indexing, and scaling of all of the data sets were performed using programs *Denzo* and *Scalepack*.[43] The structures were solved by direct methods and subsequent Fourier analyses[44] and refined by the full-matrix least-squares method based on F^2 with all of the observed reflections.[44] A difference Fourier map in **3** revealed the presence of 3.5 molecules of chloroform in the asymmetric unit. The contribution of hydrogen atoms at calculated positions were included in the final cycles of refinement. All of the calculations were performed using the *WinGX System*, version 1.70.01.[45]

Computational Methods

The electronic structures of the systems considered in this work were obtained by solving the Kohn−Sham (KS) equations, according to the density functional theory formalism.[46] The *ADF* program,[47] which solves the KS equations with the standard LCAO implementation, was employed. The following basis sets belonging to the *ADF* database were adopted: Ruthenium TZP frozen core 3d; chlorine and sulfur DZP frozen core 2p; carbon, nitrogen, and oxygen DZP frozen core 1s; hydrogen DZP. Such a choice has proven accurate and computationally economic in previous works on transition-metal complexes.[48] The geometries of the molecular triangle [{*trans,cis*-$RuCl_2$(dmso−S)$_2(\mu$-pyz)}$_3$] (**3**), of the molecular square [{*trans,cis*-$RuCl_2$(dmso−S)$_2(\mu$-pyz)}$_4$] (**4**), and of the corner complex *trans,cis,cis*-[$RuCl_2$-(dmso−S)$_2$(pyz)$_2$] (**6**) were minimized employing the gen-

(43) Otwinowski, Z.; Minor, W. In *Processing of X-ray Diffraction Data Collected in Oscillation Mode*; Carter, C. W., Jr., Sweet, R. M., Eds.; Methods in Enzymology, Macromolecular Crystallography, Part A; Academic Press: New York, 1997; Volume 276, pp 307−326.
(44) Sheldrick, G. M. *SHELX97, Programs for Crystal Structure Analysis (Release 97−2)*; University of Göttingen: Göttingen, Germany, 1998.
(45) Farrugia, L. J. *J. Appl. Crystallogr.* **1999**, *32*, 837−838.
(46) Parr, R. G.; Yang, W. *Density Functional Theory of Atoms and Molecules*; Oxford University Press: New York, 1989.
(47) Baerends, E. J.; Ellis, D. E.; Ros, P. *Chem. Phys.* **1973**, *2*, 41−51.
(48) Stener, M.; Calligaris, M. *J. Mol. Struct.* (*THEOCHEM*) **2000**, *497*, 91−104.

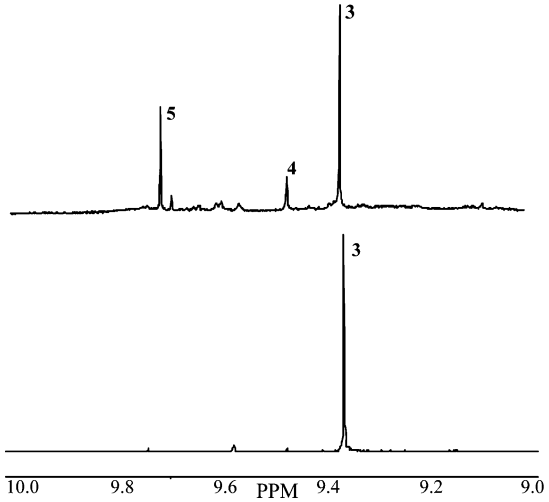

Figure 2. Downfield region of the ^{1}H NMR spectrum ($CDCl_3$) of the reaction between *trans*-[$RuCl_2$(dmso−S)$_4$] (**1**) and pyz (1:1) after 10 minutes (top) and after 2 h (bottom). The singlets originate from pyz coordinated in symmetrical environments.

eralized gradient approximation BP exchange-correlation functional.[49,50]

Results

From our previous studies, it is well-established that both *trans*-[$RuCl_2$(dmso−S)$_4$] (**1**) and *trans,cis,cis*-[$RuCl_2(CO)_2$(dmso-O)$_2$] (**2**) are suitable precursors of 90° cis bis-acceptor neutral fragments (*trans,cis*-[$RuCl_2$(dmso−S)$_2$] and *trans,cis*-[$RuCl_2(CO)_2$], respectively),[39] and we wanted to test them in self-assembly reactions with a simple linear and rigid linker such as pyrazine.

A 12 mM chloroform solution of **1**, upon the addition of an equivalent amount of pyrazine, turns from yellow to deep red-orange within a few minutes; the absorption maximum shifts from 440 to 375 nm (plus a shoulder at ca. 450 nm), with a ca. 40-fold increase in intensity. When the reaction was monitored by ^{1}H NMR spectroscopy (Experimental Section), the following observations were made: (*i*) the resonance of free pyz ($\delta = 8.59$) disappeared within minutes and was replaced by three downfield shifted singlets ($\delta =$ 9.36 (**3**), 9.49 (**4**), and 9.74 (**5**)), typical of pyz in a symmetrical environment, with an integration ratio of ca. 50 (**3**) : 15 (**4**) : 35 (**5**) (Figure 2); (*ii*) well-resolved dmso−S singlets, with 3-fold integrals, are associated to both species **3** and **4** ($\delta = 3.31$ (**3**), 3.20 (**4**)), that is, as expected for symmetrical metallacyclic species with *trans,cis*-$RuCl_2$(dmso−S)$_2$ corners and bridging pyz molecules as edges; (*iii*) the resonances of **5** and, more slowly, those of **4** disappeared with the concomitant formation of a red precipitate, probably due to polymeric species that resulted insoluble in all of the tested organic solvents (except dmso) and in water.[51]

During the first hour of the reaction, some very broad resonances in the region of pyz were observed, possibly due to oligomeric species still in solution. After 2 h, the only detectable species in solution (with sharp proton NMR signals) was **3** (Figure 2).

3 could be precipitated from these (or more concentrated) solutions upon the addition of methanol. The solutions of **3** in chloroform were substantially stable, even though they turned greenish within a few days and some additional dark-red precipitate formed, probably because of the slow hydrolysis of dmso.

Similar results, always with the concomitant formation of the precipitate, were found when the reaction between **1** and pyz was performed in refluxing chloroform (1 h) or at room temperature in other solvents (dichloromethane, nitromethane, methanol, water, acetone). Formation of the precipitate was avoided by a 4-fold reduction of the concentration of the reactants ([**1**] = [pyz] = 3 mM). In this case, the reaction being slower, some less-intense resonances for the end-on Ru-pyz species could be observed in the first minutes after the mixing of reagents. After 1 day, the only visible resonance for pyz was the singlet of **3**, but the amount of free dmso was larger than expected (i.e., more than the residual bound dmso−S). Because there was no precipitate, this implies that not all of the pyz and ruthenium is involved in the formation of **3**, and that, in solution, there must be oligomeric species containing pyz and dmso whose NMR signals are too broad to be detected.

On the basis of the above results, we anticipated that both **3** and **4** are symmetric metallacycles of formula [{*trans,cis*-$RuCl_2$(dmso−S)$_2$(μ-pyz)}$_n$], most likely a molecular triangle ($n = 3$) and a molecular square ($n = 4$). On the other hand, **5** is most likely a dinuclear intermediate, that is, [{*trans*-$RuCl_2$(dmso−S)$_3$}$_2$(μ-pyz)] or [{*trans*-$RuCl_2$(dmso−S)$_2$(H_2O)}$_2$(μ-pyz)] (the region of dmso−S resonances for this compound is not very clear because of the general low abundance of **5** and because of overlapping signals and does not allow us to determine the number of bound dmso ligands). This hypothesis is consistent with the time evolution of **5** and with the downfield shifted pyz resonance in this species. It was indeed suggested that for species in which pyz bridges diamagnetic metal fragments, the frequency of the pyz protons' resonance depends on the metal/pyz ratio; it is expected to occur more downfield in dimers, in which pyz/metal = 2, compared to metallacycles in which pyz/metal = 1.[36,52]

Treatment of **1** with a 20-fold excess of pyz led to the isolation of *trans,cis,cis*-[$RuCl_2$(dmso−S)$_2$(pyz)$_2$] (**6**).[53] The ^{1}H NMR spectrum of **6** in $CDCl_3$ consists of two doublets (4H each) at $\delta = 9.29$ and 8.57 for the two equivalent end-on pyz molecules and one singlet (12H) at $\delta = 3.28$ for the equivalent dmso−S ligands. **6** is an example of a *metal-containing ligand* and can be regarded as a good model for the corner of metallacycles **3** and **4**.

To favor the formation of the molecular square **4**, we attempted an alternative approach, that is, the reaction of **1**

(49) Becke, A. D. *Phys. Rev. A* **1988**, *38*, 3098−3100.
(50) Perdew, J. P. *Phys. Rev. B* **1986**, *33*, 8822−8824.
(51) The NMR spectrum of this precipitate in dmso-d_6, the only solvent in which it is partially soluble, shows very broad resonances exclusively.
(52) The reaction of **2** with an equimolar amount of pyrazine led initially to dinuclear and trinuclear intermediates and then to insoluble species and, for the moment, was not investigated further.
(53) Similarly, the treatment of **2** with an excess of pyz afforded the corresponding corner complex *trans,cis,cis*-[$RuCl_2(CO)_2$(pyz)$_2$] (**7**).

Scheme 4. Reaction of *trans*-[$RuCl_2$(dmso−S)$_4$] (**1**) with an Equimolar Amount of the Complementary Corner Complex *trans,cis,cis*-[$RuCl_2$(dmso−S)$_2$(pyz)$_2$] (**6**) Yielding Again the Neutral Molecular Triangle [{*trans,cis*-$RuCl_2$(dmso−S)$_2$(μ-pyz)}$_3$] (**3**)

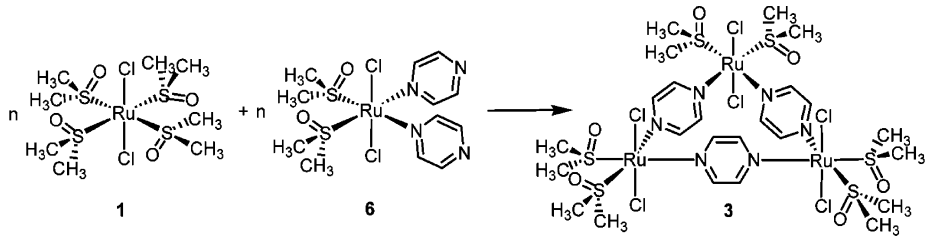

Table 2. Selected Interatomic Distances (Angstroms) and Angles (Degrees) in Molecular Triangle **3**

Ru(1)−N(1)	2.197(9)	Ru(2)−N(3)	2.156(8)	Ru(3)−N(5)	2.164(9)
Ru(1)−N(2)	2.165(8)	Ru(2)−N(4)	2.194(9)	Ru(3)−N(6)	2.161(8)
Ru(1)−S(1)	2.305(3)	Ru(2)−S(3)	2.280(3)	Ru(3)−S(5)	2.284(3)
Ru(1)−S(2)	2.248(3)	Ru(2)−S(4)	2.287(3)	Ru(3)−S(6)	2.281(3)
Ru(1)−Cl(1)	2.436(3)	Ru(2)−Cl(3)	2.435(3)	Ru(3)−Cl(5)	2.430(3)
Ru(1)−Cl(2)	2.418(3)	Ru(2)−Cl(4)	2.426(3)	Ru(3)−Cl(6)	2.453(3)
Ru(1)−Ru(2)	7.184(2)	Ru(1)−Ru(3)	7.047(2)	Ru(2)−Ru(3)	7.009(2)
N(1)−Ru(1)−N(2)	80.7(3)	N(3)−Ru(2)−N(4)	82.2(3)	N(6)−Ru(3)−N(5)	86.0(3)
S(1)−Ru(1)−S(2)	93.54(10)	S(3)−Ru(2)−S(4)	93.74(11)	S(5)−Ru(3)−S(6)	94.21(10)

with an equimolar amount of the complementary fragment **6** (Scheme 4). The reaction was performed in $CDCl_3$ at ambient temperature and monitored by ^{1}H NMR spectroscopy.

Within minutes, the resonances of the starting compounds disappeared and were replaced by those of **3** and **4** (as before, the sharp pyz singlets of the two metallacycles are accompanied by very broad and weak resonances in the pyz region). In this case, **4** was initially more abundant than **3** but gradually decreased with time (hours), and the reddish insoluble precipitate formed. After a few hours at room temperature (or ca. 1 h at 30 °C), the only species detectable in solution was again **3**. Consistent with the hypothesis that **5** is a dinuclear species, its resonances were not observed in this case.

Attempts to obtain molecular mass data through ESI-MS experiments were unsuccessful, and only mononuclear fragments could be detected. Crystals of **3** suitable for X-ray investigation were obtained from a chloroform solution by slow diffusion of *n*-hexane.

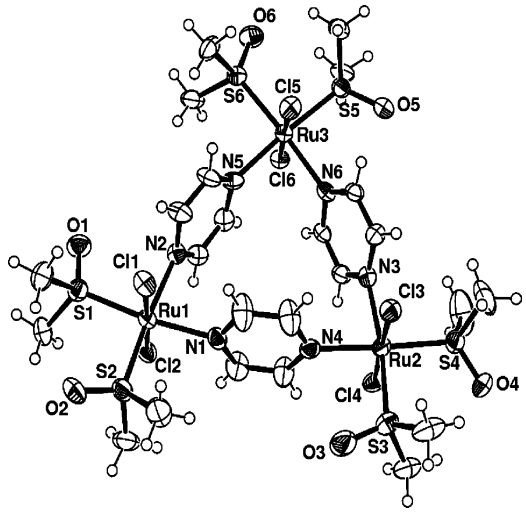

Figure 3. ORTEP drawing (50% probability ellipsoid) of molecular triangle **3** (carbon atom labels not reported for clarity).

Solid-State Structure of 3. The X-ray investigation indicated that **3** is indeed the trinuclear metallacycle [{*trans,cis*-$RuCl_2$(dmso−S)$_2$(μ-pyz)}$_3$], which is actually the first example of a neutral molecular triangle with pyrazine edges and octahedral metal corners. When redissolved in $CDCl_3$, the crystals gave the typical NMR spectrum of **3**, indicating that no isomerization had occurred during crystallization. In addition, no resonances corresponding to **4** and **5** appeared with time, confirming that **3** is stable in chloroform solution.

The ORTEP drawing of **3** is depicted in Figure 3, and a selection of bond lengths and angles is given in Table 2. The metallacycle presents a pseudo-threefold symmetry axis, and a view down this direction is evidence that all of the dmso oxygens are oriented in the same direction with each S═O bond eclipsing one of the coordination bonds in the equatorial plane. The bridging pyrazines form dihedral angles with respect to the Ru_3 plane in the range 66.0(2)−73.2(3)°, with a *syn,syn,anti* orientation. The Ru···Ru distances (side of the triangle) vary from 7.00 to 7.18 Å.

The structure analysis of **3** shows that the strain within the small metallacycle does not significantly affect the coordination geometries of the ruthenium ions, which are only slightly distorted with respect to ideal 90° angles. The largest deviations concerned, as expected, the N−Ru−N angles that fall in the range from 80.7(3) to 86.0(3)°. However, they are not significantly different from the N−Ru−N angle of 84.73(12)° found in the X-ray structure of the *corner* complex *trans,cis,cis*-[$RuCl_2$(dmso−S)$_2$(pyz)$_2$] (**6**) (below).

In the molecular triangle **3**, the largest distortions with respect to an ideal coordination geometry concern the Ru−N bonds; in fact, the pyrazine molecules, which are basically planar (the N−centroid(pyrazine)−N angles are in the range from 176.2 to 178.1°), are not linearly coordinated, but are significantly tilted as apparent from the centroid(pyrazine)−N−Ru angles that fall in the range from 165.3 to 171.9°. For comparison, in **6** these angles are 179.2 and 176.6°, that is, much closer to the ideal value of 180°.

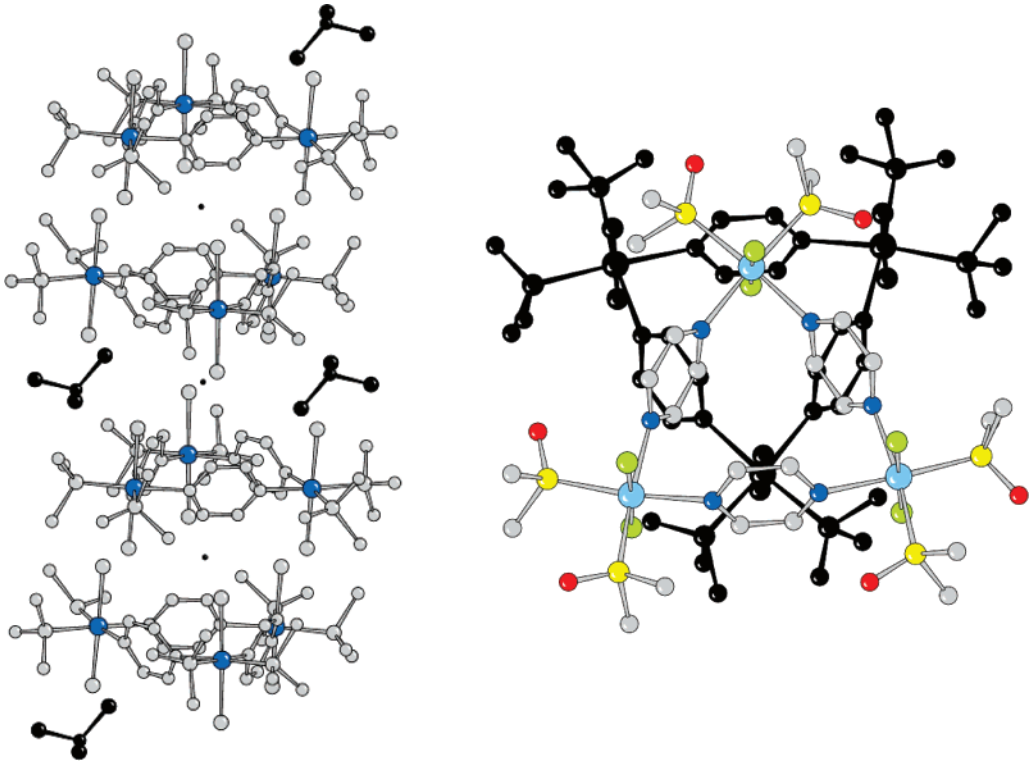

Figure 4. Left: crystal packing of **3** showing the molecular triangles piled along the *a* axis referred by centers of symmetry (small black dots, molecules of $CHCl_3$ are in black). Right: view of two stacked molecular triangles down axis *a* (bottom triangle is in black).

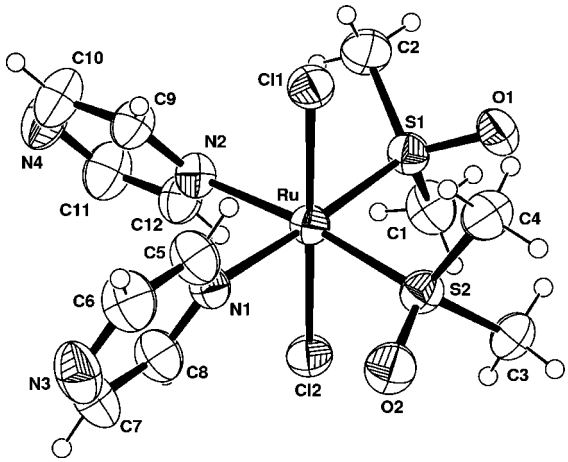

Figure 5. ORTEP drawing (40% probability ellipsoid) of *corner* complex **6** with atom labeling scheme.

The crystal packing of **3** shows that the molecular triangles stack on top of each other along the *a* axis to form columns. The stacking is antiprismatic, that is, in each column the metallacycles are related by centers of symmetry and separated alternatively by ca. 6.49 and 7.99 Å (Figure 4). The packing indicates that 37.1% of the unit cell is occupied by solvent laying in between the piled complexes, and 3.5 chloroform molecules of crystallization per each triangular unit were successfully refined.

The corner complex **6** (Figure 5) presents coordination distances (Table 3) that are overall comparable to those found in analogous Ru(II) complexes[54] and are slightly, but significantly, shorter than those measured in the molecular triangle **3** (Table 2). The S═O bonds of the two dmso−S ligands are almost coplanar with the RuS_2 plane, confirming the stereochemistry found in **3** and in other octahedral ruthenium and rhenium complexes.[55] The two pyrazine ligands form dihedral angles of 71.6(1) and 62.0(1)° with the equatorial coordination plane. As noted above, the N−Ru−N angle in **6** is similar to those found in metallacycle **3**. This geometrical feature can be mainly ascribed to the steric demand of the trans-located dmso−S ligands; in fact, in **6** the S−Ru−S angle is 93.1°, and similarly it falls within the range 93.5−94.2° in **3**. For comparison, in the corresponding corner complex in which the dmso−S ligands are replaced by the less sterically demanding CO ligands, *trans*,*cis*,*cis*-$[RuCl_2(CO)_2(pyz)_2]$ (**7**), the X-ray structure (Supporting Information) shows that the N−Ru−N angle (88.49(13)°), and correspondingly also the angle between the two *trans* ligands, OC−Ru−CO (88.0(2)°), are much closer to the ideal value of 90°.

Table 3. Selected Interatomic Distances (Angstroms) and Angles (Degrees) in *Corner* Complex **6**

Ru−N(1)	2.158(3)	Ru−S(2)	2.275(1)
Ru−N(2)	2.142(3)	Ru−Cl(1)	2.405(1)
Ru−S(1)	2.255(1)	Ru−Cl(2)	2.406(1)
N(1)−Ru−N(2)	84.75(12)	N(2)−Ru−Cl(1)	89.44(9)
N(1)−Ru−S(1)	176.50(9)	N(2)−Ru−Cl(2)	89.80(9)
N(1)−Ru−S(2)	88.25(9)	S(1)−Ru−S(2)	93.11(4)
N(1)−Ru−Cl(1)	90.97(8)	S(1)−Ru−Cl(1)	85.75(4)
N(1)−Ru−Cl(2)	90.30(8)	S(1)−Ru−Cl(2)	92.96(4)
N(2)−Ru−S(1)	94.01(9)	S(2)−Ru−Cl(1)	92.99(4)
N(2)−Ru−S(2)	172.63(9)	S(2)−Ru−Cl(2)	87.92(4)
		Cl(1)−Ru−Cl(2)	178.46(4)

(54) Alessio, E.; Iengo, E.; Zangrando, E.; Geremia, S.; Marzilli, P. A.; Calligaris, M. *Eur. J. Inorg. Chem.* **2000**, 2207−2219.

(55) Calligaris, M.; Carugo, O. *Coord. Chem Rev.* **1996**, *153*, 83−154.

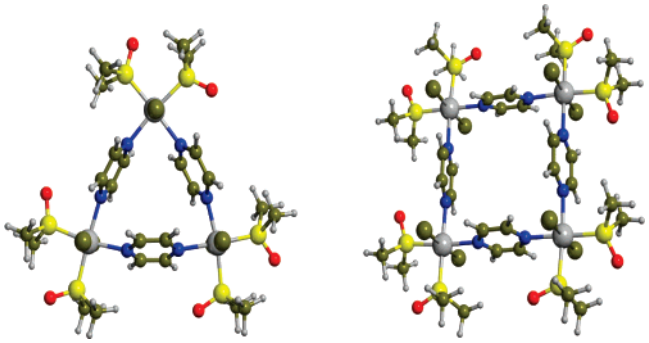

Figure 6. Calculated optimized geometries of molecular triangle **3** and molecular square **4**.

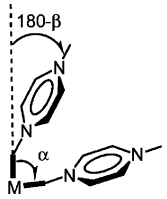

Figure 7. Schematic representation of the distortions that affect the N−Ru−N (α) and the centroid(pyrazine)−N−Ru (*β*) angles.

Calculations. In an attempt to rationalize the surprising stability of molecular triangle **3**, calculations were performed on this species, on corner complex **6**, and on the hypothetical molecular square [{*trans,cis*-$RuCl_2$(dmso−S)$_2$(*μ*-pyz)}$_4$] (**4**). The calculated geometrical parameters of **3** (Figure 6), and in particular the averaged mean N−Ru−N (83.1°) and centroid(pyrazine)−N−Ru (168.2°) angles, are in excellent agreement with those determined by X-ray crystallography (above). As expected, the corresponding angles calculated for molecular square **4** (88.1 and 178.6°, respectively; Figure 6) are closer to the ideal values. On the contrary, the calculated structure for corner complex **6** does not fit very well with the crystallographic structure, because all of the angles are closer to the ideal values; for example, the calculated N−Ru−N angle is 88.2°, compared with 84.73-(12)° found experimentally.

The X-ray diffraction data evidenced that the main distortions in the molecular triangle concern the N−Ru−N (α) and the centroid(pyrazine)−N−Ru (*β*) angles. To assess the energetics involved in these distortions with respect to the ideal coordination, we have performed calculations on modified structures of **6**, in which both α and *β* were systematically varied (Figure 7) and the energy differences with respect to the minimum value were calculated.

The results, represented as energy profiles with respect to the two angles (Figure 8), show that indeed variations of the tilt angle *β* are much-less energy demanding than those concerning distortions of the N−Ru−N angle α. To give a more-quantitative description of such effects, we have plotted in the lower panel of Figure 8 the energy as a function of the square angle, obtaining an excellent linear relationship, which indicates that harmonic profiles, $E = 1/2k_1(\Delta\alpha)^2$ and $E = 1/2k_2(\Delta\beta)$,[2] are actually found for both distortions. The linear regressions provide the values for the force constants, $k_1 = 0.154$ and $k_2 = 0.024$ kcal mol^{-1} degrees^{-1}, showing that α is over six times more rigid than *β*.

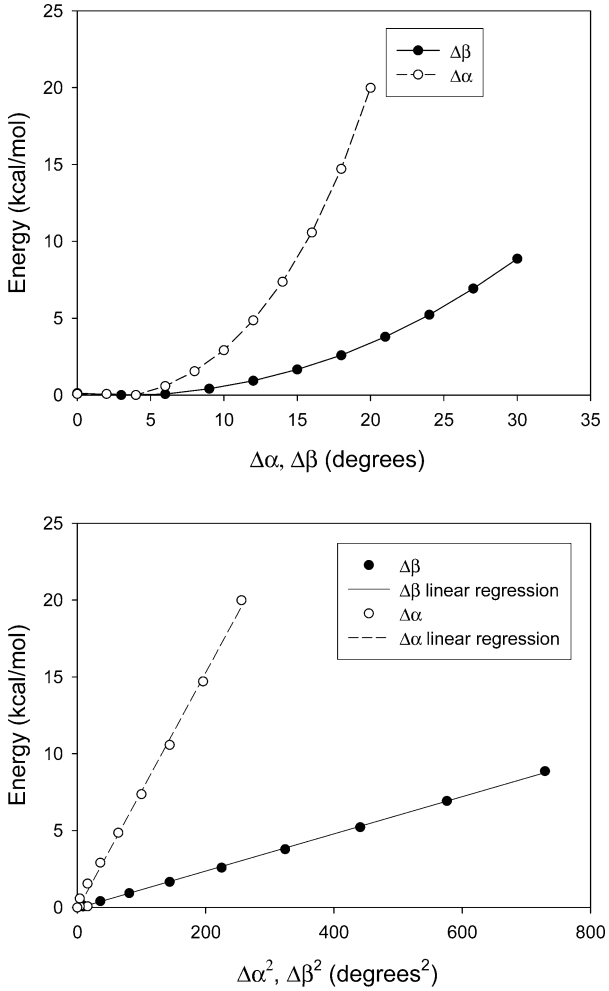

Figure 8. Upper panel: calculated energetic profile of **6** as a function of the variation of the tilt angle of pyrazine (Δ*β*, filled circles) and of the N−Ru−N angle (Δα, hollow circles). Lower panel: calculated energetic profile of **6** as a function of the square angle for both distortions.

The internal energy difference involved in the reaction 4 Δ ⇔ 3□ was calculated to be −14.4 kcal/mol in favor of the square, which means 0.6 kcal *per fragment*. This large calculated difference is not unexpected because, as noted above, calculations were unable to reproduce well the geometry of corner fragment **6**. The X-ray structures suggest that much of the enthalpic toll for the distortion of the N−Ru−N angle has been *already paid for* in the synthesis of **6** and should not contribute to a large extent to the formation of the trinuclear metallacycle **3**. In addition, internal energy cannot be employed as a stability argument, because entropic effects are completely neglected. In particular, the contribution of solvent entropy is expected to be quite significant, but it is hard to assess.

Discussion

It is now evident that the *directional bonding approach*,[5] which rationalizes the metal-mediated construction of supramolecular assemblies, allows for several exceptions. For example, quite often the combination of 90° cis bis-acceptor metal fragments with linear linkers leads to mixtures of molecular squares and triangles, rather than to the expected molecular squares only. However, the *exclusive* formation

Scheme 5. Self-Assembly of a 90° Angular Metal Fragment with the Complementary 90° Angular Corner Complex (*Metal-Containing Ligand*) to Yield a Molecular Square

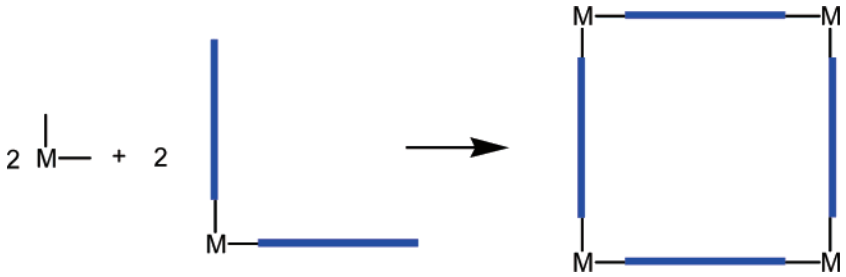

Table 4. Relevant Geometrical Parameters in Molecular Triangles with Pyrazine Edges

metal (compound)	Ru(II) (**3**)	Rh(I) (**8**)	Pt(II) (**9**)	Zn(II)[a] (**10**)
M···M (Å)	7.009, 7.047, 7.184	6.955, 6.993, 6.994	6.937, 6.944, 6.949	7.391
M···opposite pyz centroid (Å)	6.336, 6.674, 6.757,	6.356, 6.517, 6.467	6.408, 6.409, 6.487	6.872
N−M−N (deg)	80.7, 82.2, 86.0	80.5, 81.4, 81.8	82.0, 82.1, 83.2	81.6
X−M−X[b] (deg)	93.5, 93.7, 94.2	95.5, 97.4, 97.6	93.8, 94.2, 95.3	100.9
N−pyz centroid−N (deg)	175.97−178.13	177.88−179.91	178.14−178.55	177.32
M−N−pyz centroid (deg)	165.28−171.90	165.56−172.77	167.08−171.62	167.97
pyz mean plane/M3 (deg)	66.0, 68.3, 73.2	84.5, 84.8, 88.1	86.0, 86.8, 88.4	89.2
ref	present work	20	21	19

[a] The complex has a crystallographic C_3 symmetry with metals connected by the 2,5-bis(2-pyridyl)pyrazine ligand. [b] X is the ligand donor atom located trans to pyrazine (sulfur in **3**, phosphorus in **8** and **9**, chlorine in **10**).

of molecular triangles from this combination of building blocks, in particular with short inflexible linkers, is a rare and unexpected event. A remarkable example was reported by Cotton and co-workers in the course of their extensive investigation of metallacycles obtained by self-assembly of dinuclear metal fragments with bridging dicarboxylates. When in 1999 the molecular triangle [{Rh_2(DArF)$_2$(μ_4-C_2O_4)}$_3$] (DArF = *N*,*N*′-diarylformamidinate), rather than the expected molecular square, was selectively obtained with oxalate, that is, the shortest and stiffest of all dicarboxylates, Cotton wrote: *"we simply do not know why this strained triangular structure, cf. the bowed oxalate bridge, is ever adopted rather than the expected square one"*.[23]

As mentioned in the Introduction, pyrazine, which is the shortest and most-rigid linear aromatic linker is, *in principle*, the less prone to make molecular triangles when reacted with cis bis-acceptor metal corners. We found instead that the reaction between pyrazine and the neutral 90° angular precursor **1** yields, in a number of different experimental conditions, the neutral molecular triangle [{*trans*,*cis*-$RuCl_2$-(dmso−S)$_2$(μ-pyz)}$_3$] (**3**) (Scheme 3) together with polymeric material. The reaction is accompanied by the formation of transient species and, in particular, of another symmetrical metallacycle, most likely the corresponding molecular square [{*trans*,*cis*-$RuCl_2$(dmso−S)$_2$(μ-pyz)}$_4$] (**4**). Compound **4** is, however, unstable in solution, whereas the molecular triangle is stable and could be isolated and crystallized.

Quite remarkably, similar results were obtained also from the reaction between the two preformed complementary angular fragments, **1** and **6** (Scheme 4). The prevailing formation of metallacycle **4** in the initial stage of this reaction is consistent with the hypothesis that **4** is a molecular square. In fact, the two complementary angular fragments **1** and **6** have a higher degree of predisposition to give a molecular square, compared to **1** and pyz. In addition, formation of the molecular square is favored also on entropic terms, because in this case only four rather than eight fragments have to be assembled (Scheme 5).

However, the rapid formation of molecular triangle **3** from the mixture of **1** and **6** suggests that some pyz ligand must rapidly dissociate from **6** (even though no signal for free pyz was observed in the NMR spectrum). In both cases, the gradual disappearance of the resonances of **4** seems to be concomitant with the formation of the precipitate (polymeric material).

There are in the literature already two previous examples of molecular triangles that are formed *quantitatively* upon the reaction of pyrazine with 90° angular metal fragments. In each case, the metal corner is a 2+ square-planar fragment, either Rh(I) in [{Rh(PPh_3)$_2$(μ-pyz)}$_3$](ClO_4)$_3$ (**8**)[20] or Pt(II) in [{Pt(PEt_3)$_2$(μ-pyz)}$_3$](CF_3SO_3)$_6$ (**9**).[21] Another strictly related example concerns the zinc molecular triangle [{$ZnCl_2$-(PPh_3)$_2$(μ-bppz)}$_3$] (**10**, bppz = 2,5-bis(2-pyridyl)pyrazine):[19] in this metallacycle, the edges of the triangle are occupied by pyrazine moieties, whereas each pyridyl group makes an additional axial bond with a zinc corner. All of these molecular triangles have been structurally characterized in the solid state by X-ray crystallography.[19−21] The solution NMR spectra of **8** and **9** are consistent with the structures found in the solid state, even though other symmetrical metallacycles cannot be excluded.

Selected geometrical parameters for these four systems are compared in Table 4. The metal···metal distances in **8** and **9** are closely comparable (6.94−6.99 Å), although slightly shorter than those measured in **3** (7.00−7.18 Å). On the other hand, the metal···metal distances are significantly longer in the zinc metallacycle **10**, most likely to allow metal coordination by the axial pyridyl groups of bppz. It is worth noting that in **8**−**10** the pyrazine moieties are roughly coplanar, and their planes are almost perpendicular to the M_3 plane (range of dihedral angles 84−89°). On the contrary, in metallacycle **3** such dihedral angles are much smaller (66−

73°), probably because of the octahedral coordination of the ruthenium corners rather than of packing effects.

In all of the cases the N−M−N angles are smaller than the ideal value of 90°, but not to such an extent to account, *alone*, for the formation of a triangle rather than a square. The pyrazine linkers are, as expected, almost perfectly flat. The largest distortions from the ideal coordination geometry concern, in all cases, the coordination bonds of pyrazine, which are not linear, as evidenced by the centroid(pyrazine)−N−M angles, which are always considerably smaller that the ideal value of 180°.

Nevertheless, in other similar cases, even with the same metal ions, molecular squares with pyz edges are formed *exclusively*. If we exclude the case of Ti(II),[38] in which the geometry of the metal center can be considered as tetrahedral, in all of the other examples involving late transition metals we note that molecular squares are formed, both with square planar and octahedral metal corners, when the ancillary ligands on the metal coordination plane have a low steric demand: ethylenediammine in $[\{Pt(en)(\mu\text{-pyz})\}_4](NO_3)_8$,[33] ammonia in $[\{Pt(NH_3)_2(\mu\text{-pyz})\}_4](NO_3)_8$,[34] CO in [{*fac*-$ReCl(CO)_3(\mu\text{-pyz})\}_4$],[35] and [{*fac*-$ReBr(CO)_3(\mu\text{-pyz})\}_4$][36] and cyclen in $[\{(cyclen)Ru(\mu\text{-pyz})\}_4]$[37] (cyclen = 1,4,7,10-tetraazacyclododecane). We note that the hard or soft nature of the ancillary ligands seems to be less relevant in influencing the nature of the resulting pyz metallacycle.

Ferrer and co-workers similarly observed that, for linear linkers longer than pyz, the nature of the ancillary ligand on the metal corners plays a decisive role in influencing the nuclearity of the preferred metallacycle:[15] square planar $Pd(en)^{2+}$ or $Pt(en)^{2+}$ corners yield preferentially molecular squares, sometimes in equilibrium with the corresponding triangles, whereas $Pd(bipy)^{2+}$ or $Pt(bipy)^{2+}$ corners afford the molecular triangles or square/triangle mixtures.

On the basis of all of these results, we believe that the preferential formation of the molecular triangle with pyrazine edges instead of the corresponding square is determined by at least two concomitant factors: (*i*) the presence of relatively bulky ancillary ligands in the coordination plane induces a spontaneous contraction of the coordination angle at the metal corner, that is, the metal fragment is already spontaneously predisposed to be the corner of a triangle rather than of a square. The average $N_{pyz}-M-N_{pyz}$ angle is still much larger than 60° required for an equilateral triangle, but nevertheless it is narrower than the ideal value of 90° for a square. Only a minor energetic contribution is associated to this geometrical parameter in going from the corner complex to the molecular triangle. On the contrary, a widening of the $N_{pyz}-M-N_{pyz}$ angle for the formation of the molecular square would require a large energy token, as evidenced by our calculations for the $N_{pyz}-Ru-N_{pyz}$ angle. Interestingly, the X-ray structure of $[Pt(NH_3)_2(pyz)_2](NO_3)_2$, the corner complex corresponding to the molecular square $[\{Pt(NH_3)_2(\mu\text{-pyz})\}_4](NO_3)_8$,[34] shows that the $N_{pyz}-Pt-N_{pyz}$ angle is very close to 90° (as in the metallacycle), that is, in this case the corner complex is geometrically predisposed to give a square rather than a triangle, and the formation of the triangle would require a remarkable narrowing of the $N_{pyz}-Pt-N_{pyz}$ angle. (*ii*) Our calculations show that the pyz−Ru coordination bond tolerates a remarkable degree of tilting with a modest increase in strain.[56] The sum of these two relatively small distortions makes the triangle geometrically possible with a moderate enthalpic loss.

As previously noted by Cotton,[25] when the self-assembly process is under thermodynamic control, if the enthalpic token paid to the distortions that occur in the formation of the molecular triangle (i.e., the loss of the directional preferences of the components) is lower than the entropic gain, the smaller metallacycle will prevail.

Conclusions

The metallacycle $[\{trans,cis\text{-}RuCl_2(dmso-S)_2(\mu\text{-pyz})\}_3]$ (**3**) is the first example of a *neutral* molecular triangle with octahedral (rather than square-planar) metal corners and pyrazine edges. It was selectively obtained (together with polymeric material) from the reaction of the neutral 90° angular precursor *trans*-$[RuCl_2(dmso-S)_4]$ (**1**) either with pyrazine, in a number of different experimental conditions, or with the complementary corner fragment *trans,cis,cis*-$[RuCl_2(dmso-S)_2(pyz)_2]$ (**6**). Taken together, these results suggest that the molecular triangle is both the thermodynamic and the kinetic product of the reactions described above.

The X-ray structure of **3** shows that the main distortions in the molecular triangle concern the N−Ru−N and the centroid(pyrazine)−N−Ru angles, that are smaller than the ideal values of 90 and 180°, respectively. Similar distortions were found also in previous examples of cationic molecular triangles with pyz edges and Rh(I) or Pt(II) corners.[20,21] However, a N−Ru−N angle remarkably smaller than 90° was found also in the molecular structure of the strain-free corner complex **6**. We attributed this distortion in **6** to the steric demand of the trans-located dmso−S ligands.

Calculations performed on **6** indicated that it is much harder (ca. six times) to change the N−Ru−N angle than the centroid(pyrazine)−N−Ru angle, that is, the coordination geometry of pyrazine is rather flexible.

The structural and theoretical findings on **3** and **6**, together with the previous examples of molecular triangles and squares with cis-protected metal corners and linear pyz edges, suggest that the entropically favored molecular triangles might be preferred over the expected molecular squares when pyz binds to metal corner fragments, such as *trans,cis*-$RuCl_2(dmso-S)_2$, that spontaneously favor $N_{pyz}-M-N_{pyz}$ angles narrower than 90° due to the presence of ancillary ligands with significant steric demand on the coordination plane. The rather-flexible coordination geometry of pyrazine can accommodate the moderate distortions from linearity required to close the small metallacycle with modest additional strain. On the other hand, such corner fragments might prevent the formation of the corresponding molecular squares owing to

(56) Similar distortions of the coordination directions were found in the X-ray structure of a molecular triangle with the short rigid linker imidazolate and Cu(II) corners, see: Chaudhuri, P.; Karpenstein, I.; Winter, M.; Butzlaff, C.; Bill, E.; Trautwein, A. X.; Flörke, U.; Haupt, H.-J. *J. Chem. Soc., Chem. Commun.* **1992**, 321−322.

the energy token required for widening the rigid $N_{pyz}-M-N_{pyz}$ angle to almost 90°.

Acknowledgment. M.U.R. (FIRB project 2006) is gratefully acknowledged for financial support and Engelhard Italiana S.p.A. for a generous loan of hydrated $RuCl_3$. The CNR staff at ELETTRA (Trieste) are acknowledged for help in the use of the facility supported by CNR and by Elettra Scientific Division. This work was performed within the frame of COST Action D31.

Supporting Information Available: ORTEP drawing and selected interatomic distances and angles for the corner complex *trans*,*cis*,*cis*-$[RuCl_2(CO)_2(pyz)_2]$ (**7**). X-ray crystallographic data in CIF format for the structures reported in this paper. This material is available free of charge via the Internet at http://pubs.acs.org.

IC7019507